Hindawi
Wireless Communications and Mobile Computing
Volume 2019, Article ID 4946298, 10 pages
https://doi.org/10.1155/2019/4946298

Research Article

Performance Analysis of Full-Duplex Amplify-and-Forward Relay System with Hardware Impairments and Imperfect Self-Interference Cancellation

Ba Cao Nguyen and Xuan Nam Tran

Le Quy Don Technical University, Hanoi, Vietnam

Correspondence should be addressed to Xuan Nam Tran; namtx@mta.edu.vn

Received 27 February 2019; Revised 16 July 2019; Accepted 25 July 2019; Published 25 August 2019

Academic Editor: Wessam Ajib

In this paper, we analyze the performance of a full-duplex (FD) amplify-and-forward (AF) relay system with imperfect hardware. Besides the aggregate hardware impairments of the imperfect transceiver, we also consider the impact of residual self-interference (RSI) due to imperfect cancellation at the FD relay node. An analytical framework for analyzing the system performance including exact outage probability (OP), asymptotic OP, and approximate symbol error probability (SEP) is developed. In order to tackle these impacts, we propose an optimal power allocation scheme which can improve the outage performance of the FD relay node, especially at the high signal-to-noise ratio (SNR) regime. Numerical results are presented for various evaluation scenarios and verified using the Monte Carlo simulations.

1. Introduction

The fourth industrial revolution (a.k.a Industry 4.0) is developing rapidly and foreseen to have a big impact on all social and economic aspects. In the Industry 4.0 era, wireless communications will play a key role in providing broadband connections for up to tens of billions of Internet of Things (IoT) devices. While existing technologies are hardly capable of meeting the spectrum requirements for such a large number of wireless devices, the in-band full-duplex (IBFD) communication technology which can double the spectrum efficiency is a promising solution [1–11]. However, although large efforts have been made recently to produce IBFD wireless devices, it is widely known that this type of communication is still affected by residual self-interference (RSI) due to imperfect self-interference cancellation (SIC) [2–4, 12]. According to recent reports, the latest SIC techniques can achieve up to 110 dB attenuation by various methods such as isolation, wireless propagation domain suppression, and analog and digital cancellation [8, 12, 13]. The work in [14] further demonstrated that additional 36 dB attenuation can be achieved for self-interference (SI) suppression if a suitable combination of SI removal and large-scale antenna linear processing (LALP) method is used. However, more efforts still need to be done to achieve better RSI suppression.

Wireless relaying is an emerging technology which can be used to improve coverage, reliability, and spectrum efficiency has recently become a hot research topic [1, 3–11, 15–17]. It is also expected to be widely employed for the IoT networks to support machine-to-machine (M2M) communications, in which wireless relaying is an important application. Recent researches have focused on analyzing the performance of the IBFD relay networks as well as proposing advanced solutions for performance improvement. The works in [3–5, 9–11, 15] investigated performance of the IBFD amplify-and-forward (AF) one-way relay system. In [3, 4], a joint relay and transmit/receive antenna mode selection scheme was proposed. The authors derived the closed-form expressions of outage probability (OP), average symbol error rate (SER), and ergodic capacity for this system. An adaptive power allocation scheme to avoid the

outage floor was also proposed for the system. In [5], asymptotic expressions of OP and SER were derived for the FD-AF relay system. The authors also proposed optimal power allocation and relay location to minimize SER and reduce performance saturation. The work in [9] evaluated performance of an FD-AF cooperative communication system working over the Nakagami-*m* channel. The obtained results showed that this system could achieve certain gain depending on the relay processing delay, packet length, and the direct link gain. In [10], an FD-AF relay system with multiple transmit/receive antennas was investigated. The paper derived the self-interference matrix at the relay and proposed beam-forming schemes to maximize the signal-to-interference-plus-noise power ratio (SINR), thus improving the system performance. The works [11, 15] analyzed the impact of hardware impairment at the relay node on the system performance.

To improve the spectral efficiency, the FD two-way (TW) relay system was proposed and investigated in [1, 6–8, 16, 17]. The work in [1] was proposed to optimize an achievable rate with multiple relays combining with joint relay and antenna selection to obtain better signal-to-noise ratio (SNR) gain. In [6], an AF relay system consisting of multiple pairs of FD users with a single massive shared-antenna array at the FD-AF relay was considered. Optimal power allocation under user' total power constraint was proposed to maximize both spectral and energy efficiency. In [7], a multiuser FD-AF relay system with users prepairing was proposed. The paper presented the exact closed-form OP for this system and analyzed the impact of RSI on the OP performance. Besides the FD-AF-TW relay system, the FD-decode-and-forward (DF)-TW relay system was also considered widely in the literature such as in [8, 16, 17]. The exact OP for the system was derived for the case with perfect and imperfect channel state information (CSI) combined with imperfect SIC in [8, 16]. Optimal power allocation and optimal relay node placement were proposed to minimize the system OP. In [17], the spectrum efficiency (SE) of the FD-DF relay system was investigated using the sum rate as a function of the distance between the terminal and the relay node. It was shown that the system performance greatly depended on the interference suppression capability and location of the relay node.

The above overview showed that the outage performance of the FD relay systems suffered an outage floor in the high SNR regime and optimal power allocation could be used to improve the system performance and avoid such outage floor. However, most previous studies have been done for the ideal hardware systems except those in [11, 15, 18]. These works considered an additional impact of imperfect hardware but only at the relay node. In fact, the impact of imperfect hardware comes from not only the relay but also other network devices such as the source and the destination node. In practical systems, the impairment of the transceiver hardware cannot be avoided due to manufacturing imperfection, especially in the average-quality hardware components. At the transmitter, hardware impairment creates the distortion noise that causes a mismatch between the intended and transmitted signal. At the receiver, the incident signal will be distorted by the distortion during reception. The receiver is also influenced by its imperfection manufacturing such as phase oscillator noise, IQ-imbalance, and receiver filters. Large efforts were made to design compensation schemes at both the transmitter and receiver to reduce these impacts using analog and digital signal processing. However, measurement results after all compensation schemes in [19–23] showed that that the residual impairments still exist as an additive distortion noise source. In [19, 21–24], the authors considered hardware imperfection at both the transmitter and receiver using an aggregate level of impairments. Their results demonstrated that hardware impairments deteriorated the system performance and caused an irreducible floor in the OP curve. These works, however, were only done on the half-duplex systems. For FD systems, the impact of the residual impairments on the system performance becomes stronger [25], especially when considering the total hardware impairments from all nodes in the system.

Motivated by the previous results, in this paper, we consider an IBFD-AF relay system under impacts of imperfect SIC at the IBFD relay node and hardware impairments at all nodes. We intend to develop an analytical framework for analyzing its performance. The contributions of this paper can be summarized as follows:

(i) A system model of the IBFD-AF relay system under the aggregate impacts of hardware impairments at all nodes together with imperfect SIC at the relay node is developed for performance analysis. Unlike the work in [26] where the authors considered only the system achievable rate, we focus on finding the analytical expressions for OP, SEP, and the exact optimal value for transmit power at the FD relay.

(ii) The exact expressions of signal-to-interference-plus-noise-and-distortion ratio (SINDR) and OP are derived. The closed-form expression of the approximate OP is then deduced for numerical calculations. In order to gain insights into the system behaviour, we also derived the asymptotic symbol error probability (SEP).

(iii) An optimal power allocation scheme for the IBFD relay node is proposed to improve the system performance, especially in the high SNR regime.

(iv) Finally, numerical results are presented for various evaluation scenarios and verified using the Monte Carlo simulations.

The rest of the paper is organized as follows: Section 2 describes the system model. Section 3 presents performance analysis of the system in terms of OP and SEP. The optimal power allocation scheme is presented in Section 4. Numerical results and discussions are given in Section 5, and finally, Section 6 draws the conclusion of the paper.

2. System Model

Consider a typical FD-AF relay system depicted in Figure 1, which is comprised of two terminal nodes S_1 and S_2 and a

relay R. The two terminal nodes S_1 and S_2 operate in the HD mode, while relay R in the FD mode. It is also assumed that the two terminal nodes use one antenna for both transmission and reception, while the relay has two separate antennas: one for transmission and one for reception. It is worth noting that the relay R can also use one shared antenna for both transmission and reception if a circulator is used [27]. However, using separate antennas allows for better self-interference cancellation through the nature isolation, directional antenna, and cross polarization [13]. Although DF was proved to provide better performance, AF relaying is used in this paper to reduce the processing delay and hardware complexity at the relay. In the ideal case with perfect hardware and no distortion and residual SIC, the received signal at the relay R at time slot t is given as

$$y_{\mathrm{R}}(t) = h_{1\mathrm{R}} x_1(t) + z_{\mathrm{R}}(t), \tag{1}$$

where $x_1(t)$ is the transmitted signal from the source node S_1 to the relay R; $h_{1\mathrm{R}}$ denotes the fading coefficient of the channel from S_1 to R; and $z_{\mathrm{R}}(t)$ is the additive white Gaussian noise (AWGN) at the relay node with zero mean and variance σ_{R}^2, i.e., $z_{\mathrm{R}} \sim \mathcal{CN}(0, \sigma_{\mathrm{R}}^2)$.

In the case of nonideal hardware, impairment occurs at both the transmitter and receiver, resulting in distortion noises. The received signal at the relay node is now expressed as

$$y_{\mathrm{R}}(t) = h_{1\mathrm{R}}\left[x_1(t) + \eta_t^{\mathrm{S}_1}(t)\right] + \eta_r^{\mathrm{R}}(t) + z_{\mathrm{R}}(t), \tag{2}$$

where $\eta_t^{\mathrm{S}_1}(t)$ and $\eta_r^{\mathrm{R}}(t)$ denote the distortion noises due to the transmitter hardware impairment at S_1 and the receiver hardware impairment at R, respectively. These distortion noises are modeled using complex Gaussian variables as follows: $\eta_t^{\mathrm{S}_1}(t) \sim \mathcal{CN}(0, (k_t^{\mathrm{S}_1})^2 P_1)$ and $\eta_r^{\mathrm{R}} \sim \mathcal{CN}(0, (k_r^{\mathrm{R}})^2 P_1 |h_{1\mathrm{R}}|^2)$; $k_t^{\mathrm{S}_1}$ and k_r^{R} represent the level of the hardware impairments in the transmitter and the receiver, respectively. For a given channel $h_{1\mathrm{R}}$, the aggregate distortion at the relay node is given by

$$\mathbb{E}_{\eta_t^{\mathrm{S}_1}, \eta_r^{\mathrm{R}}}\left\{\left|h_{1\mathrm{R}}\eta_t^{\mathrm{S}_1} + \eta_r^{\mathrm{R}}\right|^2\right\} = P_1 |h_{1\mathrm{R}}|^2 \left[\left(k_t^{\mathrm{S}_1}\right)^2 + \left(k_r^{\mathrm{R}}\right)^2\right], \tag{3}$$

where $\mathbb{E}\{\cdot\}$ denotes the expectation operator. Equation (3) shows that the aggregate distortion at the relay node depending on the average signal power $P_1 = \mathbb{E}\{|x_1|^2\}$, the instantaneous channel gain $|h_{1\mathrm{R}}|^2$, and the impairment levels $(k_t^{\mathrm{S}_1})^2$ and $(k_r^{\mathrm{R}})^2$. Setting $k_1^2 = (k_t^{\mathrm{S}_1})^2 + (k_r^{\mathrm{R}})^2$, the aggregate distortion at the relay node becomes

$$\mathbb{E}_{\eta_t^{\mathrm{S}_1}, \eta_r^{\mathrm{R}}}\left\{\left|h_{1\mathrm{R}}\eta_t^{\mathrm{S}_1} + \eta_r^{\mathrm{R}}\right|^2\right\} = P_1 |h_{1\mathrm{R}}|^2 k_1^2, \tag{4}$$

where k_1 is the aggregate impairment level which accounts for both transmitter hardware impairment at S_1 and the receiver hardware impairment at R. For example, the aggregate level ranges from 0.08 to 0.175 for the long-term evolution (LTE) system (Section 14.3.4 in [28]).

Using (4), equation (2) is now rewritten as follows:

$$y_{\mathrm{R}}(t) = h_{1\mathrm{R}}\left[x_1(t) + \eta_1(t)\right] + z_{\mathrm{R}}(t), \tag{5}$$

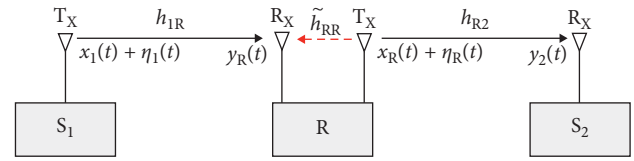

Figure 1: System model of the FD-AF one-way relay network with transceiver impairments.

where $\eta_1(t)$ describes hardware impairment at both the transmitter S_1 and the receiver R with $\eta_1 \sim \mathcal{CN}(0, k_1^2 P_1)$. Similarly, the hardware impairment aggregated at the transmitter R and the receiver S_2 is η_{R}. In the case the system has perfect CSI, η_{R} is defined as η_1, meaning $\eta_{\mathrm{R}} \sim \mathcal{CN}(0, k_{\mathrm{R}}^2 P_{\mathrm{R}})$. Herein, k_{R} is the aggregate level of impairments from the transmitter hardware k_t^{R} at R and the receiver hardware $k_r^{\mathrm{S}_2}$ at S_2, and P_{R} is the transmit power at R.

The received signal at the relay node can be rewritten as follows:

$$y_{\mathrm{R}}(t) = h_{1\mathrm{R}}\tilde{x}_1(t) + \tilde{h}_{\mathrm{RR}}\tilde{x}_{\mathrm{R}}(t) + z_{\mathrm{R}}(t), \tag{6}$$

where $\tilde{x}_1(t) \triangleq x_1(t) + \eta_1(t)$, $\tilde{x}_{\mathrm{R}}(t) \triangleq x_{\mathrm{R}}(t) + \eta_{\mathrm{R}}(t)$, and $\tilde{x}_1(t)$ and $\tilde{x}_{\mathrm{R}}(t)$ are the actual transmitted signals from two nodes S_1 and R. When $k_1 = k_{\mathrm{R}} = 0$, this system becomes an ideal one. When SIC is used to suppress the self-interference for the FD mode, RSI at the relay node $\tilde{h}_{\mathrm{RR}}\tilde{x}_{\mathrm{R}}$ reduces to I_{R}. It is also known that RSI can be modeled as a complex Gaussian-distributed variable with zero mean and variance of σ_{RSI}^2 [2, 5, 29–32], i.e., $\sigma_{\mathrm{RSI}}^2 = \tilde{\Omega}_{\mathrm{R}} P_{\mathrm{R}}$ with $\tilde{\Omega}_{\mathrm{R}}$ denoting the SIC capability. Therefore, equation (6) can be rewritten as follows:

$$y_{\mathrm{R}}(t) = h_{1\mathrm{R}}\tilde{x}_1(t) + I_{\mathrm{R}} + z_{\mathrm{R}}(t). \tag{7}$$

For the FD mode, at the same time slot t, the relay node R transmits its signal to S_2, which is based on the previously received signal. We assume that the delay due to the signal processing is equal one symbol period. Thus, the transmit signal at R is given as

$$\tilde{x}_{\mathrm{R}}(t) = G y_{\mathrm{R}}(t-1) + \eta_{\mathrm{R}}(t-1), \tag{8}$$

where G is the variable gain of the relay when the system has perfect CSI. The value of G is selected such that the transmit power of the relay node equals P_{R}, that is,

$$\mathbb{E}\left\{\left|x_{\mathrm{R}}(t)\right|^2\right\} = G^2 \mathbb{E}\left\{\left|y_{\mathrm{R}}(t-1)\right|^2\right\} = P_{\mathrm{R}}. \tag{9}$$

The relaying gain is defined as follows:

$$G \triangleq \sqrt{\frac{P_{\mathrm{R}}}{\rho_1 P_1\left(1 + k_1^2\right) + \sigma_{\mathrm{RSI}}^2 + \sigma_{\mathrm{R}}^2}}, \tag{10}$$

where $\rho_1 = |h_{1\mathrm{R}}|^2$.

The received signal at the destination node S_2 is given as

$$y_2(t) = h_{\mathrm{R}2}\tilde{x}_{\mathrm{R}}(t) + z_2(t), \tag{11}$$

where $h_{\mathrm{R}2}$ is the fading coefficient of the link from R to S_2 and $z_2(t)$ is AWGN at the destination node, $z_2 \sim \mathcal{CN}(0, \sigma_2^2)$. Using (6), (8), and (10), the received signal at the destination node can be given as

$$y_2(t) = h_{R2}G\{h_{1R}[x_1(t-1)+\eta_1(t-1)] + I_R + z_R(t-1)\} + h_{R2}\eta_R(t-1) + z_2(t). \tag{12}$$

The end-to-end signal-to-interference-plus-noise-and-distortion ratio (SINDR) is determined as follows:

$$\gamma = \frac{|h_{1R}|^2|h_{R2}|^2G^2P_1}{|h_{1R}|^2|h_{R2}|^2G^2k_1^2P_1 + |h_{R2}|^2G^2(\sigma_{RSI}^2+\sigma_R^2) + |h_{R2}|^2k_R^2P_R + \sigma_2^2} = \frac{\rho_1\rho_2P_1P_R}{\rho_1\rho_2P_1P_Rd + (\rho_2P_Rd_2+\sigma_2^2)(\sigma_{RSI}^2+\sigma_R^2) + \rho_1P_1\sigma_2^2d_1}, \tag{13}$$

where $d \triangleq k_1^2 + k_R^2 + k_1^2k_R^2$, $d_1 \triangleq 1 + k_1^2$, and $d_2 \triangleq 1 + k_R^2$.

3. Performance Analysis

3.1. Outage Probability (OP). In this section, we derive the exact OP expression of the system under the impact of hardware impairments and fading Rayleigh channel. For the AF relay system, OP is defined as the achievable rate of the system, which falls below the minimum data rate that the system must achieve. Assume that the minimum required data rate for the system is $\mathscr{R}$ and then OP can be defined as follows:

$$P_{out} = \Pr\{C < \mathscr{R}\}, \tag{14}$$

where $C = \log_2(1+\gamma)$ with γ and $\mathscr{R}$ being SINDR and the minimum required data rate of the system, respectively. Therefore, OP becomes

$$P_{out} = \Pr\{\gamma < x\}, \tag{15}$$

where $x = 2^{\mathscr{R}} - 1$.

3.1.1. Exact OP. From equation (15), OP is derived using the following theorem.

Theorem 1. *The exact OP expression of the IBFD-AF relay system in the case of both imperfect SIC and imperfect hardware under the Rayleigh fading channel is determined as follows:*

$$P_{out} = \begin{cases} 1 - 2e^{-(Ax/(1-xd))}\sqrt{\dfrac{B(x+x^2)}{(1-xd)^2}}K_1\left(2\sqrt{\dfrac{B(x+x^2)}{(1-xd)^2}}\right), & x < \dfrac{1}{d}, \\ 1, & x \geqslant \dfrac{1}{d}, \end{cases} \tag{16}$$

where
$A \triangleq (((\sigma_{RSI}^2+\sigma_R^2)d_2)/(\Omega_1P_1)) + ((\sigma_2^2d_1)/(\Omega_2P_R))$, $B \triangleq ((\sigma_2^2(\sigma_{RSI}^2+\sigma_R^2))/(\Omega_1\Omega_2P_1P_R))$, $\Omega_1 = \mathbb{E}\{|h_{1R}|^2\}$, $\Omega_2 = \mathbb{E}\{|h_{R2}|^2\}$, *and* $K_1(\cdot)$ *denotes the first-order modified Bessel function of the second kind.*

Proof. From (15), we have

$$P_{out} = \Pr\left\{\rho_1\rho_2P_1P_R(1-xd) < \left[\left(\rho_2P_Rd_2+\sigma_2^2\right)\cdot\left(\sigma_{RSI}^2+\sigma_R^2\right) + \rho_1P_1\sigma_2^2d_1\right]x\right\}. \tag{17}$$

If $(1-xd) \leqslant 0$ or $x \geqslant (1/d)$, the probability in (17) always occurs. Thus, $P_{out} = 1$. When $x < (1/d)$, we can obtain OP of the IBFD-AF relay system as follows:

$$P_{out} = 1 - \int_0^\infty \left[1 - F_{\rho_1}\left(\frac{(\sigma_{RSI}^2+\sigma_R^2)xd_2}{P_1(1-xd)} + \frac{\sigma_2^2(\sigma_{RSI}^2+\sigma_R^2)(x+x^2)}{P_1P_Ry(1-xd)^2}\right)\right] \times f_{\rho_2}\left(y + \frac{\sigma_2^2xd_1}{P_R(1-xd)}\right)dy. \tag{18}$$

In this expression, we have changed variable by letting $\rho_2 = y + (\sigma_2^2xd_1/P_R(1-xd))$, $F_\rho(\cdot)$ is the cumulative distribution functions (CDF) of ρ, and $f_\rho(\cdot)$ is the probability density function (PDF) of ρ. It is noted that, for the Rayleigh fading channel, CDF of the channel gains $\rho_l = |h_l|^2, l = 1/2$, is given by

$$F_{\rho_l}(x) = 1 - e^{-(x/\Omega_l)}, \quad x \geqslant 0, \tag{19}$$

where $\Omega_l = \mathbb{E}\{|h_l|^2\}$. After some mathematical manipulations and using expression 3.324.1 in [33], we can obtain OP of the IBFD-AF relay system given in (16). Proof of the theorem is provided in Appendix. □

3.1.2. Asymptotic OP. In order to have a better insight into the behaviour of the system under impact of hardware impairments, we derive the asymptotic OP using the assumption that the transmit power is extremely large. In the high SNR regime, $((B(x+x^2))/(1-xd)^2) \ll 1$ and $(Ax/(1-xd)) \longrightarrow 0$, using the approximation $K_1(u) \approx (1/u)$ when $u \ll 1$ [34] combining with the Taylor expansion $e^{-v} \approx 1 - v$ when $v \longrightarrow 0$, the approximate OP is derived as follows:

$$P_{out}^{ap} \approx \begin{cases} 1 - e^{-(Ax/(1-xd))}, & x < \dfrac{1}{d}, \\ 1, & x \geqslant \dfrac{1}{d}, \end{cases} \approx \begin{cases} \dfrac{Ax}{1-xd}, & x < \dfrac{1}{d}, \\ 1, & x \geqslant \dfrac{1}{d}. \end{cases} \tag{20}$$

In addition, when SNR goes to infinity and with the assumption that RSI is very small, we have

$$\lim_{SNR\longrightarrow\infty} P_{out} = \begin{cases} 0, & x < \dfrac{1}{d}, \\ 1, & x \geqslant \dfrac{1}{d}. \end{cases} \tag{21}$$

Note that, in this paper, the SNR is defined as SNR = $(\Omega_1P_1/\sigma_R^2) = (\Omega_2P_R/\sigma_2^2)$. When the hardware impairments become large, $1/d$ becomes small. Therefore, the system cannot operate with a high threshold of x because x must be smaller than $1/d$ to avoid the case of $P_{out} = 1$. As the result,

the hardware impairments limit the data transfer rate of the system.

3.2. Symbol Error Probability (SEP). SEP of the system is defined as follows [35]:

$$\text{SEP} = \alpha\mathbb{E}\left\{Q\left(\sqrt{\beta\gamma}\right)\right\} = \frac{\alpha}{\sqrt{2\pi}}\int_0^\infty F\left(\frac{t^2}{\beta}\right)e^{-\left(t^2/2\right)}dt, \quad (22)$$

where α and β are constants and their values are determined based on the modulation scheme. In wireless systems, we have $\alpha = 2$ and $\beta = 1$ when the quadrature phase-shift keying (QPSK) and 4-quadrature amplitude modulation (4-QAM) modulations are used and $\alpha = 1$ and $\beta = 2$ for the binary phase-shift keying (BPSK) modulation [35]. $Q(x) = (1/\sqrt{2\pi})\int_x^\infty e^{-(t^2/2)}dt$ is the Q-function; $F(x)$ is CDF of SINDR. Based on the definition of CDF, we can replace $F(x)$ in (22) by P_{out}, where P_{out} is determined using (16) and γ is the SINDR at the destination of the considered system.

Theorem 2. *The SEP expression of the system is determined as follows:*

$$\text{SEP} \approx \frac{\alpha\sqrt{\beta}A}{2\sqrt{2\pi(Cd)^3}}\left[\frac{\sqrt{\pi}}{2}\text{erf}\left(\sqrt{C}\right) - \sqrt{C}\exp\left(-C\right)\right] + \frac{\alpha}{2}\left[1 - \text{erf}\left(C+1\right)\right], \quad (23)$$

where $C = (\beta/2\,d) - 1$ *and* $erf(\cdot)$ *is the error function:* $erf(z) = (2/\sqrt{\pi})\int_0^z e^{-t^2}dt$.

Proof. For derivation convenience, we set $x = (t^2/\beta)$, and equation (22) becomes

$$\text{SEP} = \frac{\alpha\sqrt{\beta}}{2\sqrt{2\pi}}\int_0^\infty \frac{e^{(-\beta x/2)}}{\sqrt{x}}F(x)dx. \quad (24)$$

Using again the Taylor expansion $e^{-v} \approx 1 - v$ when $v \longrightarrow 0$, we have

$$F(x) = P_{\text{out}} \approx \begin{cases} \dfrac{Ax}{1-xd}, & x < \dfrac{1}{d}, \\ 1, & x \geqslant \dfrac{1}{d}, \end{cases} \approx \begin{cases} Axe^{(xd)}, & x < \dfrac{1}{d}, \\ 1, & x \geqslant \dfrac{1}{d}, \end{cases} \quad (25)$$

Thus, equation (24) becomes

$$\text{SEP} = \frac{\alpha\sqrt{\beta}}{2\sqrt{2\pi}}\int_0^\infty \frac{e^{-(\beta x/2)}}{\sqrt{x}}F(x)dx \approx \frac{\alpha\sqrt{\beta}}{2\sqrt{2\pi}}\left[\int_0^{1/d} Ae^{((d-\beta)/2)x}\sqrt{x}\,dx + \int_{1/d}^\infty \frac{e^{-(\beta x/2)}}{\sqrt{x}}dx\right]. \quad (26)$$

To calculate the first integral in (26), set $u = \sqrt{x}$; after some mathematical manipulations and using equation 3.321.5 in [33], we have

$$\int_0^{1/d} Ae^{(((d-\beta)/2)x)}\sqrt{x}\,dx = \frac{A}{\sqrt{(Cd)^3}}\left[\frac{\sqrt{\pi}}{2}\text{erf}\left(\sqrt{C}\right) - \sqrt{C}\,e^{-C}\right]. \quad (27)$$

For the second integral in (26), by using equations 3.361.1 and 3.361.2 in [33], we have

$$\int_{1/d}^\infty \frac{e^{-(\beta x/2)}}{\sqrt{x}}dx = \int_0^\infty \frac{e^{-(\beta x/2)}}{\sqrt{x}}dx - \int_0^{1/d}\frac{e^{-(-\beta x/2)}}{\sqrt{x}}dx = \sqrt{\frac{2\pi}{\beta}}\left[1 - \text{erf}\left(C+1\right)\right]. \quad (28)$$

Combining (26), (27), and (28), we have SEP as given in (23). The proof is thus complete. □

4. Optimal Power Allocation for the Relay Node

For the FD communications, the system performance reaches a saturated floor in the high SNR regime due to impact of RSI. To resolve this problem and improve the system performance, we propose optimal power allocation schemes for the relay node to minimize OP and SEP of the system, especially at the high SNR regime. Recalling OP in (16), in order to minimize OP, we need to choose the relay transmit power P_{R} according to the transmit power of the source node, the average channel gains of all links, the SIC capability, the average power of AWGN, and the aggregate level of impairments. Noted that there were some optimal power allocation schemes proposed for the AF-FD relay systems in the literature [26, 36, 37]. However, these works either only focused on the amplification coefficients or optimized power allocation for the ideal hardware systems. In contrast, our proposed scheme aims to reduce not only the impact of RSI but also that due to the hardware impairments.

The optimal value of the P_{R}^* is defined as follows:

$$P_{\text{R}}^* = \arg\min_{P_{\text{R}}} P_{\text{out}}. \quad (29)$$

From here, a step-by-step guideline to obtain the optimal value of the relay transmit power is summarized in Algorithm 1.

In order to reduce the complex calculation of the exact P_{out}, we can use $P_{\text{out}}^{\text{ap}}$ for calculating P_{R}^*, particularly in the high SNR regime. The optimal value for the relay transmit power is obtained using Theorem 3.

Theorem 3. *The optimal value* P_R^* *of the FD-AF relay system with hardware impairments is determined as follows:*

$$P_{\text{R}}^* = P_0 = \sqrt{\frac{\Omega_1 P_1 \sigma_2^2 d_1}{\Omega_2\widetilde{\Omega}_{\text{R}}d_2}}. \quad (30)$$

Proof. In the high SNR regime, OP of the system can be simply given in the first expression of (21). Taking the derivative of $P_{\text{out}}^{\text{ap}}$ with respect to P_{R} in the case $x < (1/d)$, we have

(1) Solve $(\partial P_{\text{out}}/\partial P_{\text{R}}) = 0$ for $P_{\text{R}} = P_0$;
(2) **if** $\begin{cases} P_0 > 0 \\ (\partial P_{\text{out}}/\partial P_{\text{R}}) < 0 \text{ for } P_{\text{R}} < P_0 \\ (\partial P_{\text{out}}/\partial P_{\text{R}}) > 0 \text{ for } P_{\text{R}} > P_0 \end{cases}$
(3) **then**
(4) Output optimal power $P_{\text{R}}^* = P_0$;
(5) **else**
(6) Output optimal power $P_{\text{R}}^* = \varnothing$;
(7) **end**

Algorithm 1: Optimal power calculation algorithm.

$$\frac{\partial P_{\text{out}}^{\text{ap}}}{\partial P_{\text{R}}} = \exp\left(-\frac{Ax}{1-xd}\right)\frac{x}{1-xd}\frac{\partial A}{\partial P_{\text{R}}}, \tag{31}$$

where

$$\frac{\partial A}{\partial P_{\text{R}}} = \frac{\widetilde{\Omega}_{\text{R}} d_2}{\Omega_1 P_1} - \frac{\sigma_2^2 d_1}{\Omega_2 P_{\text{R}}^2}. \tag{32}$$

Therefore, $(\partial P_{\text{out}}^{\text{ap}}/\partial P_{\text{R}}) = 0$ when $P_{\text{R}} = P_{\text{R}}^*$. For $P_{\text{R}} < P_{\text{R}}^*$, it is clear that $(\partial P_{\text{out}}^{\text{ap}}/\partial P_{\text{R}}) < 0$ and $(\partial P_{\text{out}}^{\text{ap}}/\partial P_{\text{R}}) > 0$ when $P_{\text{R}} > P_{\text{R}}^*$. Thus, $P_{\text{R}} = P_{\text{R}}^*$ is the optimal value of relay transmit power. The proof is thus complete.

It is noted that the optimal transmit power in Theorem 3 includes the distances between S_1 and R (denoted by $d_{1\text{R}}$) and between R and S_2 (denoted by $d_{\text{R}2}$). Due to the effect of large-scale fading, the variances of the channel gains $|h_{1\text{R}}|^2$ and $|h_{\text{R}2}|^2$ are related to these distance as follows: $\Omega_1 = d_{1\text{R}}^{-\alpha}$ and $\Omega_2 = d_{\text{R}2}^{-\alpha}$, where α represents the path loss exponent ($\alpha = 2, 3, \ldots, 6$) [8]. As a result, expression (30) can be used to investigate the effect of the relay relative locations on the system performance. Although it is not shown in the paper, we would like to note that this effect is similar with that observed in an ideal hardware system presented in [8]. □

5. Numerical Results

In this section, numerical results are presented to evaluate performance of the considered system. Simulation results are also used to validate the theoretical analysis. Main performance measures used for evaluation are OP, system throughput, and SEP under impact of both hardware impairment and RSI. The impact of hardware impairment is illustrated by comparing with the case of ideal hardware, i.e., $k_1 = k_{\text{R}} = 0$, for various RSI scenarios. In addition, the proposed power allocation is also applied and compared with the case without power allocation. In our simulations, the average SNR is defined as $\text{SNR} = (\Omega_1 P_1/\sigma_{\text{R}}^2) = (\Omega_2 P_{\text{R}}/\sigma_2^2)$. It is worth noting that when optimal power allocation is used, the average SNR is the SNR at the relay, i.e., $\text{SNR} = (\Omega_1 P_1/\sigma_{\text{R}}^2)$. Other parameters for simulations are chosen as follows: the average channel gains $\Omega_1 = \Omega_2 = 1$; the AWGN variance at the relay and the destination $\sigma_{\text{R}}^2 = \sigma_2^2 = 1$. Figure 2 illustrates the OP performance obtained by (16) and Monte Carlo simulations for $P_1 = P_{\text{R}}$. Two minimum required data rates are $\mathscr{R} = 2$ and $\mathscr{R} = 5$ bit/s/Hz. The investigated thresholds for OP are $x = 2^2 - 1 = 3$ and $x = 2^5 - 1 = 31$. The aggregate level of impairments is $k_1 = k_{\text{R}} = 0.1$. The SIC capability is $\widetilde{\Omega}_{\text{R}} = -30$ dB. Since $\sigma_{\text{RSI}}^2 = \widetilde{\Omega}_{\text{R}} P_{\text{R}}$, increasing the relay transmit power creates more

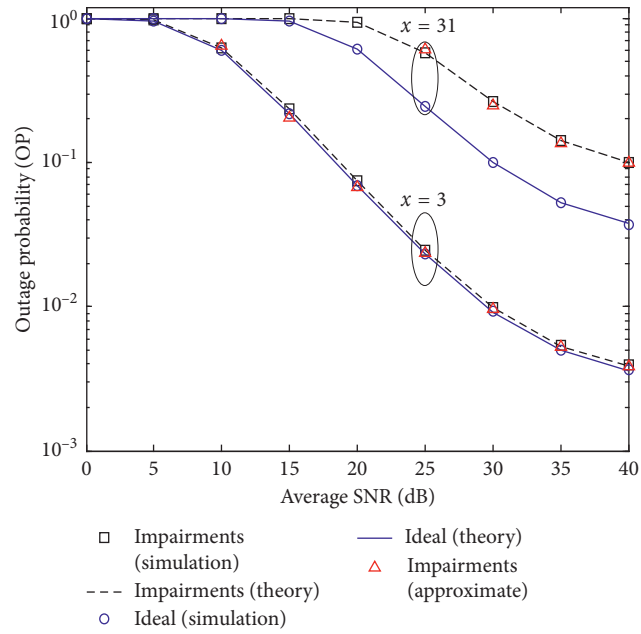

Figure 2: OP performance versus the average SNR for two thresholds $x = 3$ and $x = 31$, $k_1 = k_{\text{R}} = 0.1$, and $\widetilde{\Omega}_{\text{R}} = -30$ dB.

RSI. As can be seen in Figure 2, for the low rate system ($x = 3$), the impact of hardware impairments is trivial. But for the high rate system ($x = 31$), hardware impairments have a strong impact on the system performance. Therefore, depending on system requirements, wireless devices (network nodes) need to select a suitable transmission rate to avoid unnecessary performance loss, especially for high-rate transmission systems. It is also noted that, in the high SNR regime, the OP performance of both ideal hardware and hardware impairment systems becomes saturated to an outage floor. In such cases, the proposed optimal power allocation scheme can be applied for performance improvement.

Figure 3 compares the OP performances of the hardware-impairment system with and without optimal power allocation at the relay node for $x = 3$ and $x = 31$, $k_1 = k_{\text{R}} = 0.1$, and $\widetilde{\Omega}_{\text{R}} = -30$ dB. The optimal power is calculated using equation (30), while the nonoptimization uses $P_{\text{R}} = P_1$. The remaining parameters for simulations are the same as in Figure 2. It is clearly seen from the figure that, at SNR lower than 35 dB, the gain due to the optimal power allocation is small. But in the high SNR regime (above 35 dB), the proposed optimization can help to mitigate the outage floor caused by RSI and improve the system performance significantly, particularly when SNR > 40 dB. It is worth noting that we have used all system parameters to derive the relay optimal transmit power, and thus the proposed optimization does mitigates not only the RSI impact but also other factors such as hardware impairments, relay location, and AWGN in the system. Note also that the optimal power for the ideal hardware system is given by setting $k_1 = k_{\text{R}} = 0$ in (30).

Figure 4 plots OP of the system versus the distortion factor k for SNR = 40 dB, $\widetilde{\Omega}_{\text{R}} = -30$ dB, and $\mathscr{R} = 2, 3, 4$, and 5 bit/s/Hz. In the figure, the distortion factors are chosen as $k_1 = k_{\text{R}} = k$. As observed from the figure, the impact of hardware impairment on the low-rate transmission

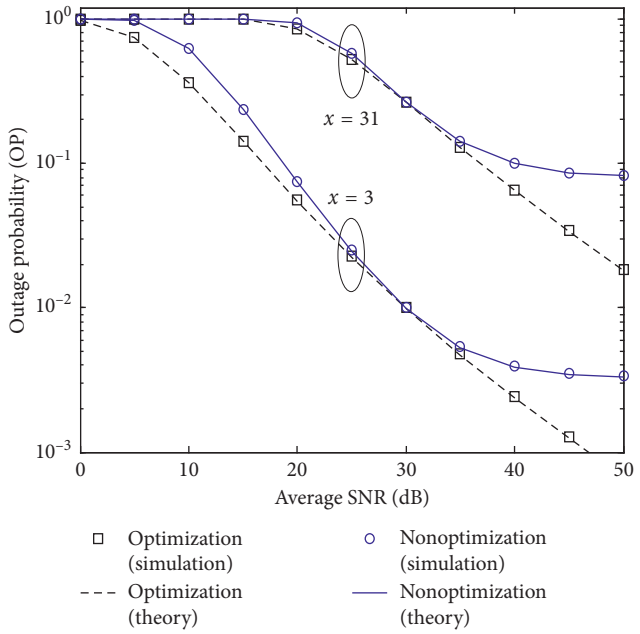

FIGURE 3: OP performance versus the average SNR for the case with and without optimal power allocation for $x = 3$ and $x = 31$, $k_1 = k_R = 0.1$, and $\tilde{\Omega}_R = -30$ dB.

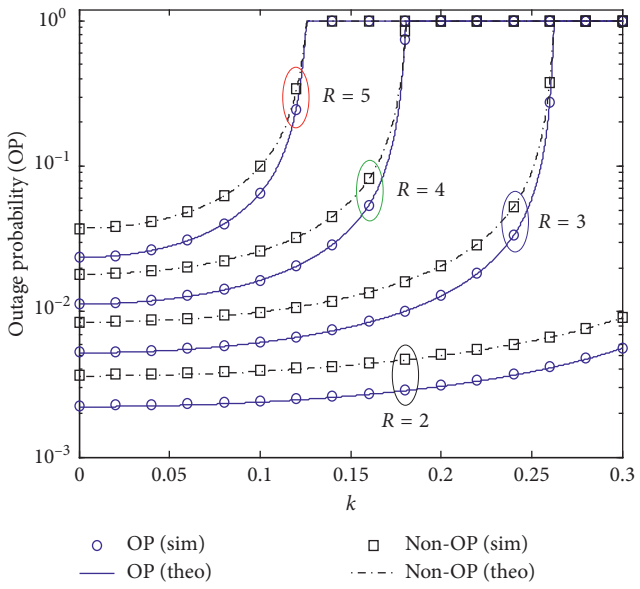

FIGURE 4: OP performance versus the distortion factor k with and without optimization; SNR = 40 dB, $\tilde{\Omega}_R = -30$ dB, and $\mathscr{R} = 2, 3, 4,$ and 5 bit/s/Hz.

system ($\mathscr{R} = 2$ and 3 bit/s/Hz) with small distortion factors is trivial. However, this impact becomes more significant for the high-rate system ($\mathscr{R} = 4$ and 5 bit/s/Hz) even when the distortion factor is small ($k = 0.1$). With $k > 0.1$ and $\mathscr{R} = 4$ and 5 bit/s/Hz, the outage performance decreases quickly; however, the proposed optimal power allocation still shows significant improvement over the nonoptimal one.

Figure 5 shows the OP performance versus both the distortion factor k and RSI for the case with optimization. The OP is a function (denoted by g) of both variables k and

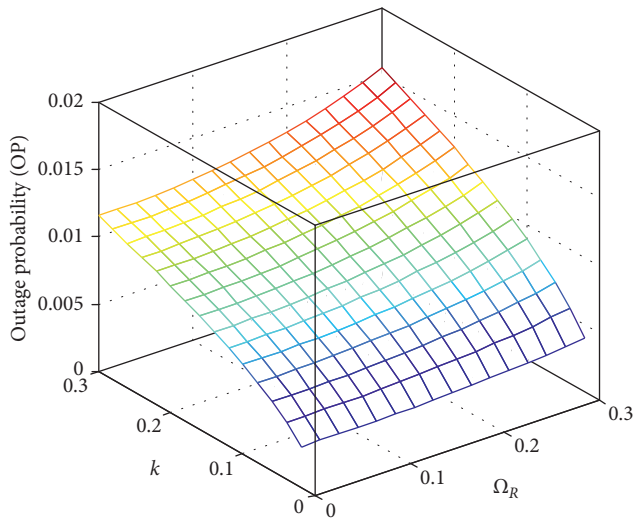

FIGURE 5: OP performance versus both distortion factor k and RSI with optimization: SNR = 40 dB and $\mathscr{R} = 1$ bit/s/Hz.

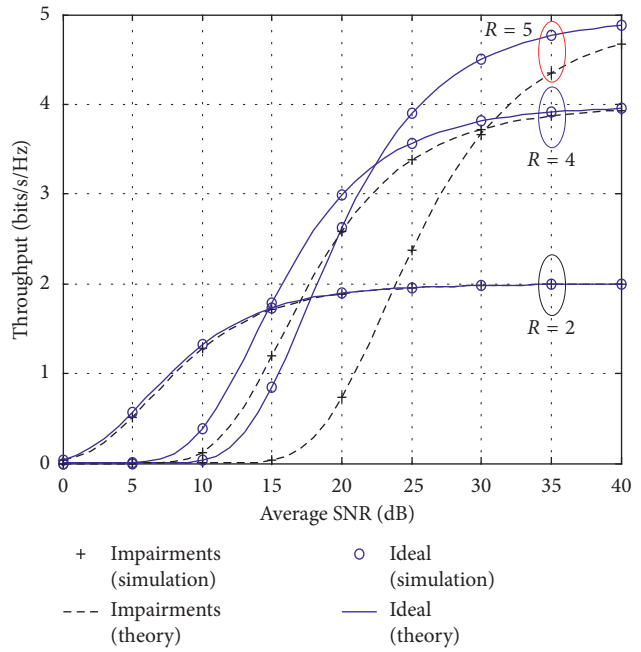

FIGURE 6: System throughput versus the average SNR with optimal power allocation for $\mathscr{R} = 2, 4,$ and 5 bit/s/Hz, $k_1 = k_R = 0.1$, and $\tilde{\Omega}_R = -30$ dB.

$\tilde{\Omega}_R$, i.e., OP $= g(k, \tilde{\Omega}_R)$. We can see from the figure that when $k = 0$ and $\tilde{\Omega}_R = 0$, the performance of the considered system becomes that of the HD system with ideal hardware. In this case, we have OP $= g(0, 0) = 3.10^{-4}$. Similarly, when $k \neq 0$ and $\tilde{\Omega}_R = 0$, the considered system becomes the HD system with hardware impairments. In this case, the OP performance is the same with that in [24]. In the case that $k = 0$ and $\tilde{\Omega}_R \neq 0$, the considered system becomes the ideal FD system. As can be seen from Figure 5, the impact of the hardware impairments is stronger than that of the RSI causing the OP performance degradation due to k to increase faster than that due to $\tilde{\Omega}_R$. For examples, we have $g(0.02, 0.1) = 0.0031$, while $g(0.1, 0.02) = 0.0066$. Since the

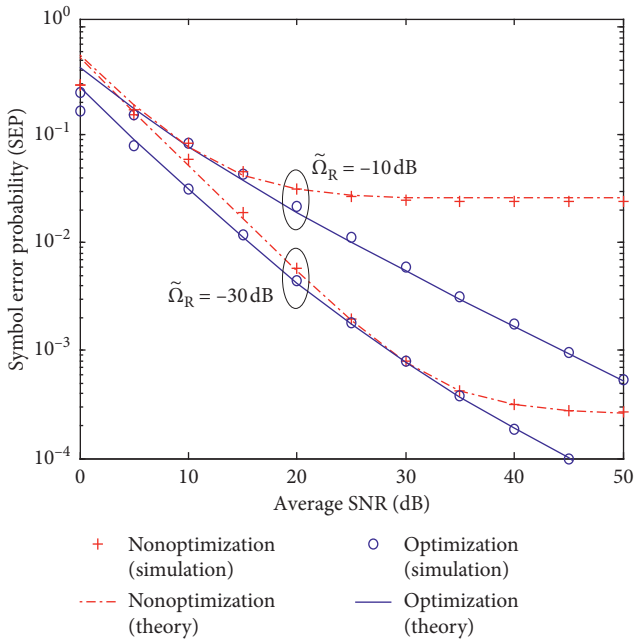

FIGURE 7: SEP performance versus the average SNR with and without optimal power allocation and $\widetilde{\Omega}_R = -10$ and -30 dB and $k_1 = k_R = 0.1$.

optimal transmit power is used at the FD relay, the impact of RSI on the OP performance decreases significantly compared with that of the HI one.

Figure 6 compares throughput of the ideal and nonideal hardware system with power optimization for $\mathscr{R} = 2, 4,$ and 5 bit/s/Hz, $k_1 = k_R = 0.1$, and $\widetilde{\Omega}_R = -30$ dB. The system throughput is defined as $\mathscr{T} = \mathscr{R}(1 - P_{out})$. As can be seen from the figure, for low-rate systems ($\mathscr{R} = 2$), the system throughput soon reaches the target rate at SNR = 25 dB. For high-rate systems, it requires a higher SNR to reach the target ($\mathscr{R} = 4$ when SNR = 40 dB and $\mathscr{R} = 5$ when SNR > 40 dB).

Finally, Figure 7 illustrates the SEP performance of the system with different values of the SIC capability, $\widetilde{\Omega}_R = -10, -30$ dB and $k_1 = k_R = 0.1$, using BPSK modulation and with and without optimal power allocation. In the figure, the theory curve is plotted using numerical results obtained from (23). It can be noticed that there is a good agreement between the numerical and simulation results, especially in the high SNR regime. It is also obvious that when RSI is strong ($\widetilde{\Omega}_R = -10$ dB), the SEP performance soon becomes saturated at about SNR = 20 dB if optimization is not used. When RSI is smaller than $\widetilde{\Omega}_R = -30$ dB, the SEP floor appears later (at about SNR = 35 dB). Therefore, in order to reduce the complex design of the FD transceivers, wireless designers can select suitable relay transmit power according to the RSI level obtained by measurements after all SIC techniques. For example, for $\widetilde{\Omega}_R = -10$ dB, optimal power allocation must be used, but when $\widetilde{\Omega}_R = -30$ dB, if the system requires SEP = 10^{-3} at SNR = 35 dB, the FD transceiver does not require power optimization. For SNR > 35 dB if the system needs to improve performance, power optimization can be applied for this case.

6. Conclusion

In the paper, we analyzed the impacts of the hardware impairments and RSI on performance of the IBFD-AF relay system. Using mathematical analysis, we successfully obtained the exact and asymptotic OP, the SEP of the system. The system performance was then analyzed for various scenarios of SNR, RSI, and hardware impairments. Both numerical and simulation results showed a strong impact of RSI and hardware impairments on the system performance. The proposed optimal power allocation scheme can improve the system performance significantly. However, when the system is affected more by hardware impairment and RSI, only optimal power allocation cannot guarantee required performance. Other advanced solutions should be considered to be included in the system.

Appendix

This appendix provides the detailed derivation of the exact OP expression in Theorem 1.

Note that the OP is a function of two variables ρ_1 and ρ_2 as presented in (17). By applying the law of conditional probability [38], the OP can be calculated as

$$P_{out} = \Pr\{\gamma < x\} = \int_0^\infty \Pr\{\gamma < x|_{\rho_2}\} f_{\rho_2}(\rho_2)\partial\rho_2. \quad \text{(A1)}$$

In the case $x < 1/d$, by letting $\rho_2 = y + (\sigma_2^2 x d_1/(P_R(1 - xd)))$ and using (A1), the probability in (17) becomes (18).

On the contrary, the PDF of instantaneous channel gains following the Rayleigh fading distribution is given by

$$f_{\rho_l}(x) = \frac{x}{\Omega_l} e^{-(x/\Omega_l)}, \quad x \geq 0. \quad \text{(A2)}$$

Using the CDF and PDF in (19) and (A2), we have

$$F_{\rho_1}\left(\frac{(\sigma_{RSI}^2 + \sigma_R^2)xd_2}{P_1(1 - xd)} + \frac{\sigma_2^2(\sigma_{RSI}^2 + \sigma_R^2)(x + x^2)}{P_1 P_R y(1 - xd)^2}\right) = 1 - e^{-\left(\left(\left(\sigma_{RSI}^2 + \sigma_R^2\right)xd_2/\left(\Omega_1 P_1(1 - xd)\right)\right) + \left(\sigma_2^2\left(\sigma_{RSI}^2 + \sigma_R^2\right)(x + x^2)/\left(\Omega_1 P_1 P_R y(1 - xd)^2\right)\right)\right)}, \quad \text{(A3)}$$

$$f_{\rho 2}\left(y + \frac{\sigma_2^2 x d_1}{P_R(1 - xd)}\right) = \frac{1}{\Omega_2} e^{-(y/\Omega_2) + \left(\left(\sigma_2^2 x d_1\right)/\left(\Omega_2 P_R(1 - xd)\right)\right)}. \quad \text{(A4)}$$

Therefore, equation (18) becomes

$$\begin{aligned} P_{\text{out}} &= 1 - \int_0^{\infty} e^{-\left(\left(\left(\left(\sigma_{\text{RSI}}^2+\sigma_{\text{R}}^2\right)xd_2\right)/\left(\Omega_1 P_1\left(1-xd\right)\right)\right)-\left(\left(\sigma_2^2\left(\sigma_{\text{RSI}}^2+\sigma_{\text{R}}^2\right)\left(x+x^2\right)\right)/\left(\Omega_1 P_1 P_{\text{R}} y\left(1-xd\right)^2\right)\right)\right)} \\ &\quad \times \frac{1}{\Omega_2} e^{-\left(\left(y/\Omega_2\right)+\left(\sigma_2^2 xd_1/\Omega_2 P_{\text{R}}\left(1-xd\right)\right)\right)} \partial y \\ &= 1 - \frac{1}{\Omega_2} e^{-\left(\left(\left(\left(\sigma_{\text{RSI}}^2+\sigma_{\text{R}}^2\right)xd_2\right)/\left(\Omega_1 P_1\left(1-xd\right)\right)\right)-\left(\sigma_2^2 xd_1/\left(\Omega_2 P_{\text{R}}\left(1-xd\right)\right)\right)\right)} \\ &\quad \times \int_0^{\infty} e^{-\left(\left(\left(\sigma_2^2\left(\sigma_{\text{RSI}}^2+\sigma_{\text{R}}^2\right)\left(x+x^2\right)\right)/\left(\Omega_1 P_1 P_{\text{R}} y\left(1-xd\right)^2\right)\right)-\left(y/\Omega_2\right)\right)} \partial y. \end{aligned} \tag{A5}$$

Applying equation 3.324.1 in [33], we can calculate the above integral as

$$\begin{aligned} &\int_0^{\infty} e^{-\left(\left(\sigma_2^2\left(\sigma_{\text{RSI}}^2+\sigma_{\text{R}}^2\right)\left(x+x^2\right)\right)/\left(\Omega_1 P_1 P_{\text{R}} y\left(1-xd\right)^2\right)\right)-\left(y/\Omega_2\right)} \partial y \\ &= \sqrt{\frac{4\Omega_2\sigma_2^2\left(\sigma_{\text{RSI}}^2+\sigma_{\text{R}}^2\right)\left(x+x^2\right)}{\Omega_1 P_1 P_{\text{R}}\left(1-xd\right)^2}} \\ &\quad \times K_1\left(\sqrt{\frac{4\sigma_2^2\left(\sigma_{\text{RSI}}^2+\sigma_{\text{R}}^2\right)\left(x+x^2\right)}{\Omega_1\Omega_2 P_1 P_{\text{R}}\left(1-xd\right)^2}}\right). \end{aligned} \tag{A6}$$

Therefore, we obtain the OP as follows:

$$\begin{aligned} P_{\text{out}} &= 1 - \frac{1}{\Omega_2} e^{-\left(\left(\left(\left(\sigma_{\text{RSI}}^2+\sigma_{\text{R}}^2\right)xd_2\right)/\left(\Omega_1 P_1\left(1-xd\right)\right)\right)-\left(\left(\sigma_2^2 xd_1\right)/\left(\Omega_2 P_{\text{R}}\left(1-xd\right)\right)\right)\right)} \\ &\quad \times \sqrt{\frac{4\Omega_2\sigma_2^2\left(\sigma_{\text{RSI}}^2+\sigma_{\text{R}}^2\right)\left(x+x^2\right)}{\Omega_1 P_1 P_{\text{R}}\left(1-xd\right)^2}} \\ &\quad \times K_1\left(\sqrt{\frac{4\sigma_2^2\left(\sigma_{\text{RSI}}^2+\sigma_{\text{R}}^2\right)\left(x+x^2\right)}{\Omega_1\Omega_2 P_1 P_{\text{R}}\left(1-xd\right)^2}}\right) \\ &= 1 - e^{-\left(\left(\left(\left(\sigma_{\text{RSI}}^2+\sigma_{\text{R}}^2\right)xd_2\right)/\left(\Omega_1 P_1\left(1-xd\right)\right)\right)-\left(\left(\sigma_2^2 xd_1\right)/\left(\Omega_2 P_{\text{R}}\left(1-xd\right)\right)\right)\right)} \\ &\quad \times \sqrt{\frac{4\sigma_2^2\left(\sigma_{\text{RSI}}^2+\sigma_{\text{R}}^2\right)\left(x+x^2\right)}{\Omega_1\Omega_2 P_1 P_{\text{R}}\left(1-xd\right)^2}} \\ &\quad \times K_1\left(\sqrt{\frac{4\sigma_2^2\left(\sigma_{\text{RSI}}^2+\sigma_{\text{R}}^2\right)\left(x+x^2\right)}{\Omega_1\Omega_2 P_1 P_{\text{R}}\left(1-xd\right)^2}}\right) \\ &= 1 - e^{-\left(\left(x\right)/\left(1-xd\right)\right)\left(\left(\left(\left(\sigma_{\text{RSI}}^2+\sigma_{\text{R}}^2\right)d_2\right)/\left(\Omega_1 P_1\right)\right)+\left(\left(\sigma_2^2 d_1\right)/\left(\Omega_2 P_{\text{R}}\right)\right)\right)} \\ &\quad \times 2\sqrt{\frac{\sigma_2^2\left(\sigma_{\text{RSI}}^2+\sigma_{\text{R}}^2\right)\left(x+x^2\right)}{\Omega_1\Omega_2 P_1 P_{\text{R}}\left(1-xd\right)^2}} \\ &\quad \times K_1\left(2\sqrt{\frac{\sigma_2^2\left(\sigma_{\text{RSI}}^2+\sigma_{\text{R}}^2\right)\left(x+x^2\right)}{\Omega_1\Omega_2 P_1 P_{\text{R}}\left(1-xd\right)^2}}\right) \\ &= 1 - 2e^{-Ax/\left(1-xd\right)}\sqrt{\frac{B\left(x+x^2\right)}{\left(1-xd\right)^2}} K_1\left(2\sqrt{\frac{B\left(x+x^2\right)}{\left(1-xd\right)^2}}\right). \end{aligned} \tag{A7}$$

The proof is now complete.

Data Availability

The data used to support the findings of this study are included within the article.

Conflicts of Interest

The authors declare that they have no conflicts of interest.

References

[1] J. Hu, F. Liu, and Y. Liu, "Achievable rate analysis of two-way full duplex relay with joint relay and antenna selection," in *Proceedings of the 2017 IEEE Wireless Communications and Networking Conference (WCNC)*, pp. 1–5, San Francisco, CA, USA, March 2017.

[2] S. Hong, J. Brand, J. Choi et al., "Applications of self-interference cancellation in 5G and beyond," *IEEE Communications Magazine*, vol. 52, no. 2, pp. 114–121, 2014.

[3] K. Yang, H. Cui, L. Song, and Y. Li, "Joint relay and antenna selection for full-duplex AF relay networks," in *Proceedings of the 2014 IEEE International Conference on Communications (ICC)*, pp. 4454–4459, Sydney, Australia, June 2014.

[4] K. Yang, H. Cui, L. Song, and Y. Li, "Efficient full-duplex relaying with joint antenna-relay selection and self-interference suppression," *IEEE Transactions on Wireless Communications*, vol. 14, no. 7, pp. 3991–4005, 2015.

[5] S. Li, K. Yang, M. Zhou et al., "Full-duplex amplify-and-forward relaying: power and location optimization," *IEEE Transactions on Vehicular Technology*, vol. 66, no. 9, pp. 8458–8468, 2017.

[6] P. Xing, J. Liu, C. Zhai, X. Wang, and X. Zhang, "Multipair two-way full-duplex relaying with massive array and power allocation," *IEEE Transactions on Vehicular Technology*, vol. 66, no. 10, pp. 8926–8939, 2017.

[7] B. Xia, C. Li, and Q. Jiang, "Outage performance analysis of multi-user selection for two-way full-duplex relay systems," *IEEE Communications Letters*, vol. 21, no. 4, pp. 933–936, 2017.

[8] C. Li, Z. Chen, Y. Wang, Y. Yao, and B. Xia, "Outage analysis of the full-duplex decode-and-forward two-way relay system," *IEEE Transactions on Vehicular Technology*, vol. 66, no. 5, pp. 4073–4086, 2017.

[9] F. E. Airod, H. Chafnaji, and A. Tamtaoui, "Performance analysis for amplify and forward full-duplex relaying with direct link over nakagami-m fading channel," in *Proceedings of the 2017 International Conference on Wireless Networks And Mobile Communications (WINCOM)*, pp. 1–6, Rabat, Morocco, November 2017.

[10] D. Hwang, J. Yang, and S. S. Nam, "Sinr maximizing beamforming schemes for the full duplex amplify-and-forward relay channel," *IEEE Access*, vol. 5, pp. 18987–18998, 2017.

[11] O. Taghizadeh, A. C. Cirik, and R. Mathar, "Hardware impairments aware transceiver design for full-duplex amplify-and-forward MIMO relaying," *IEEE Transactions on Wireless Communications*, vol. 17, no. 3, pp. 1644–1659, 2017.

[12] A. Sabharwal, P. Schniter, D. Guo, D. W. Bliss, S. Rangarajan, and R. Wichman, "In-band full-duplex wireless: challenges and opportunities," *IEEE Journal on Selected Areas in Communications*, vol. 32, no. 9, pp. 1637–1652, 2014.

[13] M. Heino, D. Korpi, T. Huusari et al., "Recent advances in antenna design and interference cancellation algorithms for in-band full duplex relays," *IEEE Communications Magazine*, vol. 53, no. 5, pp. 91–101, 2015.

[14] P. Xing, J. Liu, C. Zhai, and Z. Yu, "Self-interference suppression with imperfect channel estimation in a shared-antenna full-duplex massive MU-MIMO system," *EURASIP Journal on Wireless Communications and Networking*, vol. 2017, no. 1, p. 18, 2017.

[15] G. J. Gonzalez, F. H. Gregorio, J. E. Cousseau, T. Riihonen, and R. Wichman, "Full-duplex amplify-and-forward relays with optimized transmission power under imperfect transceiver electronics," *EURASIP Journal on Wireless Communications and Networking*, vol. 2017, no. 1, 2017.

[16] C. Li, H. Wang, Y. Yao, Z. Chen, X. Li, and S. Zhang, "Outage performance of the full-duplex two-way DF relay system under imperfect CSI," *IEEE Access*, vol. 5, pp. 5425–5435, 2017.

[17] L. Li, C. Dong, L. Wang, and L. Hanzo, "Spectral-efficient bidirectional decode-and-forward relaying for full-duplex communication," *IEEE Transactions on Vehicular Technology*, vol. 65, no. 9, pp. 7010–7020, 2016.

[18] X. N. Tran, B. C. Nguyen, and D. T. Tran, "Outage probability of two-way full-duplex relay system with hardware impairments," in *Proceedings of the 2019 3rd International Conference on Recent Advances in Signal Processing, Telecommunications & Computing (SigTelCom)*, IEEE, pp. 135–139, Hanoi, Vietnam, March 2019.

[19] A. K. Mishra, S. C. M. Gowda, and P. Singh, "Impact of hardware impairments on TWRN and OWRN AF relaying systems with imperfect channel estimates," in *Proceedings of the 2017 IEEE Wireless Communications and Networking Conference (WCNC)*, pp. 1–6, San Francisco, CA, USA, March 2017.

[20] T. Schenk, *RF Imperfections in High-Rate Wireless Systems: Impact and Digital Compensation*, Springer Science & Business Media, Berlin, Germany, 2008.

[21] C. Studer, M. Wenk, and A. Burg, "MIMO transmission with residual transmit-RF impairments," in *Proceedings of the 2010 International ITG Workshop on Smart Antennas (WSA)*, pp. 189–196, IEEE, Bremen, Germany, February 2010.

[22] X. Zhang, M. Matthaiou, E. Bjornson, M. Coldrey, and M. Debbah, "On the MIMO capacity with residual transceiver hardware impairments," in *Proceedings of the 2014 IEEE International Conference on in Communications (ICC)*, pp. 5299–5305, IEEE, Sydney, Australia, June 2014.

[23] A. Papazafeiropoulos, S. K. Sharma, T. Ratnarajah, and S. Chatzinotas, "Impact of residual additive transceiver hardware impairments on Rayleigh-product MIMO channels with linear receivers: exact and asymptotic analyses," *IEEE Transactions on Communications*, vol. 66, no. 1, pp. 105–118, 2017.

[24] E. Bjornson, M. Matthaiou, and M. Debbah, "A new look at dual-hop relaying: performance limits with hardware impairments," *IEEE Transactions on Communications*, vol. 61, no. 11, pp. 4512–4525, 2013.

[25] D. Bharadia, E. McMilin, and S. Katti, "Full duplex radios," *ACM SIGCOMM Computer Communication Review*, ACM, vol. 43, no. 4, ACM, pp. 375–386, 2013.

[26] O. Taghizadeh, M. Rothe, A. C. Cirik, and R. Mathar, "Distortion-loop analysis for full-duplex amplify-and-forward relaying in cooperative multicast scenarios," in *Proceedings of the 2015 9th International Conference on Signal Processing And Communication Systems (ICSPCS)*, pp. 1–9, IEEE, Cairns, Australia, December 2015.

[27] P. Xing, J. Liu, C. Zhai, X. Wang, and L. Zheng, "Spectral efficiency of the in-band full-duplex massive multi-user multiple-input multiple-output system," *IET Communications*, vol. 11, no. 4, pp. 490–498, 2017.

[28] H. Holma and A. Toskala, *LTE for UMTS: Evolution to LTE-Advanced*, John Wiley & Sons, Hoboken, NJ, USA, 2011.

[29] B. C. Nguyen, X. N. Tran, and D. T. Tran, "Performance analysis of in-band full-duplex amplify-and-forward relay system with direct link," in *Proceedings of the 2018 2nd International Conference on Recent Advances in Signal Processing, Telecommunications & Computing (SigTelCom)*, pp. 192–197, IEEE, Ho Chi Minh, Vietnam, January 2018.

[30] G. Chen, P. Xiao, J. R. Kelly, B. Li, and R. Tafazolli, "Full-duplex wireless-powered relay in two way cooperative networks," *IEEE Access*, vol. 5, pp. 1548–1558, 2017.

[31] B. C. Nguyen, X. N. Tran, T. M. Hoang, and L. T. Dung, "Performance analysis of full-duplex vehicle-to-vehicle relay system over double-Rayleigh fading channels," *Mobile Networks and Applications*, vol. 19, pp. 1–10, 2019.

[32] B. C. Nguyen, T. M. Hoang, and P. T. Tran, "Performance analysis of full-duplex decode-and-forward relay system with energy harvesting over Nakagami-*m* fading channels," *AEU—International Journal of Electronics and Communications*, vol. 98, pp. 114–122, 2019.

[33] A. Jeffrey and D. Zwillinger, *Table of Integrals, Series, and Products*, Academic Press, Cambridge, MA, USA, 2007.

[34] M. Abramowitz and I. A. Stegun, *Handbook of Mathematical Functions with Formulas, Graphs, and Mathematical Tables*, Vol. 9, Dover, New York, NY, USA, 1972.

[35] A. Goldsmith, *Wireless Communications*, Cambridge University Press, Cambridge, UK, 2005.

[36] L. J. Rodriguez, N. H. Tran, and T. Le-Ngoc, "Optimal power allocation and capacity of full-duplex AF relaying under residual self-interference," *IEEE Wireless Communications Letters*, vol. 3, no. 2, pp. 233–236, 2014.

[37] O. Taghizadeh, J. Zhang, and M. Haardt, "Transmit beamforming aided amplify-and-forward MIMO full-duplex relaying with limited dynamic range," *Signal Processing*, vol. 127, pp. 266–281, 2016.

[38] A. Leon-Garcia and A. Leon-Garcia, *Probability, Statistics, and Random Processes for Electrical Engineering*, Pearson/Prentice Hall, Upper Saddle River, NJ, USA, 3rd edition, 2008.